# Noise-induced synchronous neuronal oscillations

Christian Kurrer* and Klaus Schulten
*Department of Physics and Beckman Institute, University of Illinois at Urbana-Champaign, 405 North Mathews Avenue, Urbana, Illinois 61801*
(Received 23 May 1994)

We investigate a model for synchronous neural activity in networks of coupled neurons. The individual systems are governed by nonlinear dynamics and can continuously vary between excitable and oscillatory behavior. Analytical calculations and computer simulations show that coupled excitable systems can undergo two different phase transitions from synchronous to asynchronous firing behavior. One of the transitions is akin to the synchronization transitions in coupled oscillator systems, while the second transition can only be found in coupled excitable systems. We present an analytical derivation of the two transitions and discuss implications for synchronization transitions in biological neural networks.

PACS number(s): 87.10.+e, 05.20.−y

## I. INTRODUCTION

Recently, the temporal characteristics of neuronal firing patterns have received renewed interest. This has been triggered by experiments that related firing correlation of neurons in the visual cortex to properties of the visual stimulus [1,2]. The concept of synchronous neuronal firing itself, however, is not new. Neurons in the brain tend to fire synchronously under a large variety of conditions; the very fact that macroscopic currents and potentials are recorded in EEG measurements indicates that the neurons must be involved in coherent activity [3,4].

In an attempt to understand the origin and role of synchronous neuronal activity, a number of recent modeling approaches have been based on a description of the single neuron as oscillators [5–11], firing coherency being controlled through a competition between synchronizing interactions and desynchronizing noise. However, recent computer simulation studies using coupled integrate-and-fire [12,13] or excitable neurons [14–16] have shown a second type of synchronization transition which is triggered by changes in the excitation threshold. In this paper, we provide an analytical derivation of the latter type of synchronization transitions. We will demonstrate the importance of noise added to the neuron dynamics in both destroying and generating firing coherency.

In Sec. II, we discuss the nonlinear dynamics of physiological neuron models. We will study the firing frequencies of both noiseless and noisy neurons and point out that upon change of the input parameter, noiseless neurons undergo an abrupt transition between silence and constant firing, whereas noisy neurons smoothly increase their firing frequency in this case. In Sec. III, we discuss the concept of a stochastic limit cycle, that will allow us to treat noisy excitable dynamical systems in a way similar to that of dynamical systems with limit cycle. In Sec. IV, we discuss the active rotator model, which describes the dynamics of a neuronal system along the stochastic limit cycle. In Sec. V, we derive a solution of the Fokker-Planck equation for ensembles of coupled active rotator systems. This solution will be used in Sec. VI to derive a phase diagram for the synchronous and asynchronous modes of coupled active rotators. In the concluding Sec. VII, we discuss some of the implications for the understanding of the role of synchronous neural activity that has been observed in physiological neural networks.

## II. NONLINEAR DYNAMICS OF PHYSIOLOGICAL NEURONS

The first quantitative physiological model for neuronal dynamics was formulated by Hodgkin and Huxley [17]. Their set of four coupled differential equations described the neuron as an excitable element or oscillator, depending on the value of the stimulation current. Fitzhugh [18] proposed a simplification of the Hodgkin-Huxley equations in terms of the two-dimensional Bonhoeffer–van der Pol (BvP) dynamics,

$$\begin{aligned} \dot{x_1} &= F_1(x_1,x_2) = c(x_1 - x_1^3/3 + x_2 + z), \\ \dot{x_2} &= F_2(x_1,x_2) = \tfrac{1}{c}(a - x_1 - bx_2), \end{aligned} \tag{1}$$

choosing $a$=0.7, $b$=0.8, $c$=3. The variable $x_1$ represents the transmembrane voltage, while the "recovery variable" $x_2$ represents slow ionic membrane conductivities. The parameter $z$ represents the external stimulation of the neuron: for high stimulation ($-0.34 > z > -0.875$), the system becomes an oscillator with approximately fixed frequency. The more interesting case, however, is that of low or intermediate stimulation ($0.5 > z > -0.34$), for which the system of equations (1) has a stable stationary point and represents an excitable system. In this case, random noise added to the neuron dynamics, e.g., in $x_1$, will lead to the occasional release of a single pulse. Variations of $z$, representing synaptic input, will change the height of the firing threshold and, thereby, can change the average firing rate of neurons by orders of magnitude [19,20]. (In this paper, we only discuss the effect of slow variations of

*Present address: Department of Physics, Kyoto University, Kyoto, Japan.

 

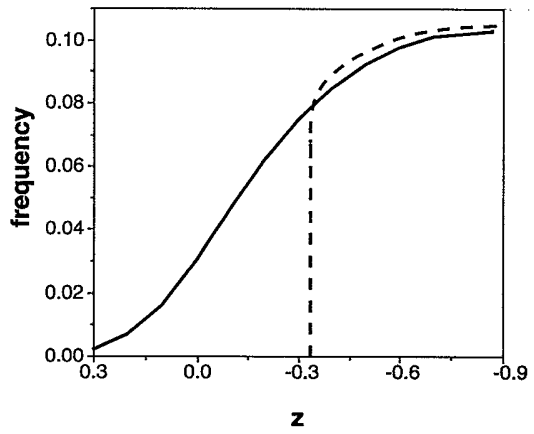


FIG. 1. Firing frequencies of BvP neurons as a function of the input parameter $z$. For noiseless BvP systems, the firing frequency jumps abruptly to a near constant value at $z = 0.34$ (broken curve). For noisy systems, the firing frequency varies continuously as a function of $z$ in a sigmoid fashion (solid curve).

the threshold on the average firing rate. For a discussion of the effect of fast variations of the threshold on the structure of the pulse train, we refer to a recent paper by Wiesenfeld *et al.* [21].)

Figure 1 shows the firing frequencies for the physiological BvP neurons as a function of the input variable $z$. In the noiseless case, the activity switches abruptly between silence and limit cycle oscillations. Moderate noise added to the BvP dynamics produces a sigmoid transition in the average firing frequency. It is important to note that the neuron is most sensitive to variations of the input $z$ in a range of $z$ ($z \approx -0.2$) where the BvP equations result in an excitable element rather than limit cycle dynamics.

In this paper, we will thus address the question of how synchronous activity can arise in networks of coupled excitable elements.

## III. STOCHASTIC LIMIT CYCLES

Investigations of coupled nonlinear oscillators are often simplified by parametrizing the limit cycle of the oscillator in terms of a phase variable [22]. One can also assign a phase to states of the oscillator that are in the vicinity of the limit cycle by projecting the states onto the limit cycle along so-called isochrones. This reduction from a multidimensional state vector to a one-dimensional phase variable for a single oscillator significantly simplifies the treatment of ensembles of coupled neurons and in many cases makes the derivation of analytical results possible [23].

When investigating excitable elements, we can use the concept of *stochastic limit cycles* to reduce a multidimensional dynamical system to a one-dimensional system described by a phaselike variable. The concept of stochastic limit cycles [19,20] stems from the observation that noise-driven excitable systems often yield dynamical behavior very similar to that of limit cycle systems. In an excitable system, noise can drive the system away from the stationary point toward an excitation threshold. After reaching the excitation threshold, the dynamical system will return to the stationary state usually after a long detour through phase space. We can then define the stochastic limit cycle for excitable systems by connecting the most likely escape trajectory out of the stationary point with the most likely return trajectory back to the stationary point. The state of systems on this circular trajectory, as well as points in its vicinity, can again be parametrized in terms of a one-dimensional phaselike variable.

## IV. STOCHASTIC ACTIVE ROTATOR NEURONS

The phase dynamics of a limit cycle oscillator can always be expressed as

$$\dot{\phi} = F(\phi) = 1 \tag{2}$$

through a suitable rescaling of the time scale. This is not the case of stochastic limit cycles. In the absence of noise, the motion along the stochastic limit cycle is not uniform; on some parts of the cycle, the deterministic dynamics would actually push the system backwards on the cycle rather than forwards. This situation of alternating positive and negative phase speed along the circular trajectory can be described in first order approximation through the modified phase dynamics,

$$\dot{\phi} = F(\phi) = 1 - a\sin(\phi), \tag{3}$$

the so-called "active rotator" model first studied in this context by Shinomoto and Kuramoto [14]. For $a > 1$, Eq. (3) yields stretches of positive and negative phase velocity like on a stochastic limit cycle, while for $a < 1$, Eq. (3) corresponds to ordinary limit cycle dynamics.

The two cases $a > 1$ and $a < 1$ yield the same qualitative behavior as the BvP model neuron for $z > -0.34$ and $z < -0.34$, respectively. In the following, we want to focus on the case $a > 1$ in which the system behaves as an excitable system. The stationary point of the active rotator dynamics is given by

$$\phi_s = \arcsin(1/a). \tag{4}$$

In the presence of Gaussian white noise, the neuron dynamics is described by

$$\dot{\phi} = F(\phi) + \eta(t), \tag{5}$$
$$\langle \eta(t_1)\eta(t_2)\rangle = 2D\delta(t_2 - t_1).$$

In this case the state of a neuron will no longer remain exactly in the stationary state [Eq. (4)]. Nonetheless, the neuron is most likely to be found in the vicinity of this stationary point, as it is driven back to $\phi_s$ after small perturbations. In the limit of small noise, the probability distribution for the state of a single neuron $i$ can be described approximately by a Gaussian function centered at the stationary point

$$p_i(\phi_i) = \frac{1}{\sqrt{2\pi}\sigma} \exp\left(-\frac{1}{2}\frac{(\phi_i - \phi_s)^2}{\sigma^2}\right) \quad (6)$$

with

$$\sigma = \sqrt{D/(a\cos\phi_s)}. \quad (7)$$

From time to time, noise will drive the system sufficiently far away from $\phi_s$ such that the neuron will no longer be attracted directly back to $\phi_s$, but rather orbit once around the stochastic limit cycle. This corresponds to the release of a single spiking event in a biological neuron. The distance that has to be overcome by noise to evoke a spike decreases as $a$ approaches 1, making such spiking events more and more likely. In this way, changes of $a$ can modulate the average firing rate in close analogy to such modulation through the parameter $z$ in the BvP model [19]. The pulse train produced by such a stochastic neuron is nevertheless very irregular (only when $a$ is lowered below 1 will the spike train become quasiperiodic).

We now consider the case of a network of coupled stochastic neurons. For the sake of simplicity, we assume that all neurons $i$ interact linearly with all other neurons $j$ ($j = 1, ..., N$) [24]

$$\dot{\phi}_i = F_i(\phi_i, \{\phi_j\}) + \eta_i(t) \quad (8)$$

$$= \left(F(\phi_i) + \frac{1}{N}\sum_j^N w_{ji}\sin(\phi_j - \phi_i)\right) + \eta_i(t).$$

The linear interactions can be superimposed and replaced by a single force pulling the neuron towards the center of mass of all other neurons. The dependence on neurons $\{\phi_j\}$ in Eq. (8) can then be replaced by a dependence on the center of mass $\phi_{\text{c.m.}}$ of the population of neurons. Moreover, we will assume that $\frac{1}{N}\sum_j w_{ij} = w$ for all $i$, i.e., all neurons are connected to the other neurons of the network by the same average synaptic strength. Under these conditions, the probability distribution $p_i(\phi_i)$ for one neuron $i$ will become representative for all other neurons, allowing a mean field description. Note that the $w_{ij}$ describe only a coupling of neurons within the network, while the effect of external input is described by changes of $a$ in $F(\phi_i)$.

For large values of $a$, the probability distribution for a single neuron is again peaked in the vicinity of the stationary point. As we lower the value of $a$, individual neurons will then fire more often, although still uncorrelated. Below a certain value $a_c > 1$, however, the probability distribution will cease to be stationary [14]; instead, its center of mass will be able to slip over the escape threshold and orbit periodically around the limit cycle. This entails that the firing pattern of neurons will make a transition from uncorrelated and aperiodic firing to correlated and periodic firing.

In order to describe this transition we have to study under what conditions a distribution of neurons can jointly escape out of an attractive basin of a stationary point. While the specific system described by Eq. (8) has been characterized numerically in earlier work [14,25], the approach outlined below allows an (approximate) analytical solution; it focuses on the escape of a distribution across a threshold and should be applicable to a general class of escape processes. While the escape of a *single* stochastic system out of a local minimum has been extensively studied and can approximately be described by the passage time formulas [26], we want here to develop a general theory describing the *coherent* escape of a distribution of interacting systems.

## V. APPROXIMATE SOLUTION OF THE FOKKER-PLANCK EQUATION FOR ACTIVE ROTATOR NEURONS

An exact description of the probability distribution would require a self-consistent solution of the Fokker-Planck equation

$$\partial_t p_i(\phi_i, t) = \left[-\partial_{\phi_i} F_i(\phi_i, \phi_{\text{c.m.}}) + D\partial^2_{\phi_i}\right] p_i(\phi_i, t) \quad (9)$$

which is not available for arbitrary $F$.

A standard approach [27] to solving Eq. (9) for localized distributions, used in [28], would be to expand $F$ in a Taylor expansion around the center of the distribution $\phi_{\text{c.m.}}$

$$F_i(\phi_i, \phi_{\text{c.m.}}) = F(\phi_{\text{c.m.}}) + (\phi_i - \phi_{\text{c.m.}})\partial_{\phi_{\text{c.m.}}} F(\phi_{\text{c.m.}}). \quad (10)$$

Using this approximation in Eq. (9), one obtains as solution a Gaussian distribution

$$p_i(\phi_i, t) = \frac{1}{\sqrt{2\pi}\sigma(t)} \exp\left(-\frac{1}{2}\frac{[\phi_i - \phi_{\text{c.m.}}(t)]^2}{\sigma^2(t)}\right), \quad (11)$$

where the motion of the center of mass and the time evolution of the width of the distribution are given by

$$\dot{\phi}_{\text{c.m.}} = F(\phi_{\text{c.m.}}), \quad (12)$$

$$\dot{\sigma^2} = 2\left[\partial_{\phi_{\text{c.m.}}} F(\phi_{\text{c.m.}}) - w\right]\sigma^2 + 2D. \quad (13)$$

In this approximation [27] the center of the Gaussian distribution would always end up in the stationary point for $t \to \infty$. To describe the escape from the stationary point, we have to take into account additional terms in the Taylor expansion Eq. (10). Accounting for terms up to second order [29], we obtain an improved version of Eqs. (12) and (13),

$$\dot{\phi}_{\text{c.m.}} = F(\phi_{\text{c.m.}}) + \frac{\sigma^2}{2}F''(\phi_{\text{c.m.}}), \quad (14)$$

$$\dot{\sigma^2} = 2\left[\partial_{\phi_{\text{c.m.}}} F(\phi_{\text{c.m.}}) - w\right]\sigma^2 + 2D. \quad (15)$$

Equation (11) together with (14) and (15) thus provides an approximate solution of the Fokker-Planck equation (9).

For distributions of finite size $\sigma > 0$, Eq. (14) can describe the escape out of a stationary point characterized by $F(\phi) = 0$. Approximating the distribution as a Gaussian distribution can be done as long as the dis-

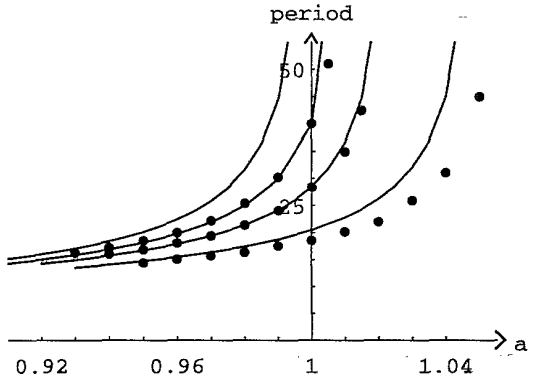


FIG. 2. Oscillation periods for the center of mass phase of ensembles of coupled active rotators. The continuous curves show the periods obtained from Eqs. (16) and (17) for $w = 1$ and $D = 0$ (top curve), 0.025, 0.05, and 0.1 (bottom curve). The three sets of dots represent periods obtained from Monte Carlo simulations of 10 000 coupled active rotators.

tribution is sharply peaked, i.e., $w \gg D$. The solution of Eq. (9) will approach an exact Gaussian in the limit where $-\frac{\partial F}{\partial \phi} + w \gg |\frac{\sigma^n}{n!}\frac{\partial^n F}{\partial^n \phi}|$ $(n > 1)$. We can then improve Eqs. (14) and (15) by averaging the values of $F$ and $\frac{\partial F}{\partial \phi}$ over the whole Gaussian distribution (11).

For coupled active rotators [Eq. (8)], averaging $F$ and $\frac{\partial F}{\partial \phi}$ over the whole distribution $p(\phi)$ yields the equations of motion

$$\dot{\phi}_{\text{c.m.}} = 1 - a\sin(\phi_{\text{c.m.}})e^{-\frac{\sigma^2}{2}}, \tag{16}$$

$$\dot{\sigma^2} = -2[a\cos(\phi_{\text{c.m.}})e^{-\frac{\sigma^2}{2}} + we^{-\sigma^2}]\sigma^2 + 2D. \tag{17}$$

In order to test the validity of the Gaussian approximation that was used to derive these equations, we integrated Eqs. (16) and (17) numerically to calculate the oscillation period of the center of mass for different parameter values and compared these predictions with results obtained from Monte Carlo simulations of 10 000 coupled active rotators. The results are shown in Fig. 2.

The distributions become exact Gaussians only in the limit $\sigma \ll 1$. Distributions with large $\sigma$ will no longer be exactly Gaussian and we can, thus, expect differences between the actual firing period and the one predicted using Eqs. (16) and (17). Deviations in predicted oscillation periods due to $\sigma \gtrsim 1$ become apparent in the bottom pair of curves of Fig. 2 for $D = 0.1$.

## VI. PHASE TRANSITIONS IN ACTIVE ROTATOR ENSEMBLES

From Eqs. (16) and (17) we can now derive boundaries in $(a, w, D)$ space for the different dynamical regimes of the solutions. First we want to determine under which condition there exists a solution in which $\dot{\phi}_{\text{c.m.}} = 0$ and $\dot{\sigma^2} = 0$ holds simultaneously. Inserting these conditions into Eqs. (16) and (17) yields

$$\sin(\phi) = \frac{1}{a}e^{\frac{\sigma^2}{2}}, \tag{18}$$

$$\sigma^2 = \frac{D}{a\cos(\phi)e^{-\frac{\sigma^2}{2}} + we^{-\sigma^2}}. \tag{19}$$

For small $\sigma$ $(D \ll w)$ and in the limit $a \ll w$, we only obtain a stationary solution if

$$a > a_c = 1 + \frac{1}{2}\frac{D}{w}. \tag{20}$$

If $a$ is larger than $a_c$, the solution will be stationary and peaked in the vicinity of the stationary point $\phi_s$. If $a$ is smaller than $a_c$ the center of mass may continuously orbit around the limit cycle. Equation (20) thus describes our first phase boundary.

Next we address whether for $a < a_c$ the width of the distribution will remain finite, corresponding to correlated firing of the neurons, or whether the width will grow without bounds, which corresponds to a probability distribution which smears out over the whole limit cycle. We, therefore, have to investigate the long time behavior of Eq. (17). By averaging Eq. (17) over one limit cycle revolution for $a \ll w$ we obtain

$$\dot{\sigma^2} = -2we^{-\sigma^2}\sigma^2 + 2D. \tag{21}$$

With $w > 0$ and $D > 0$, we can only obtain a solution $\dot{\sigma^2} = 0$ if

$$D/w \lesssim 0.736. \tag{22}$$

Equation (22) describes the approximation result for the second phase boundary. (While it is obtained through an approximation strictly valid only in the low noise limit, it is reasonably close to the numerical result $D/w = 0.5$

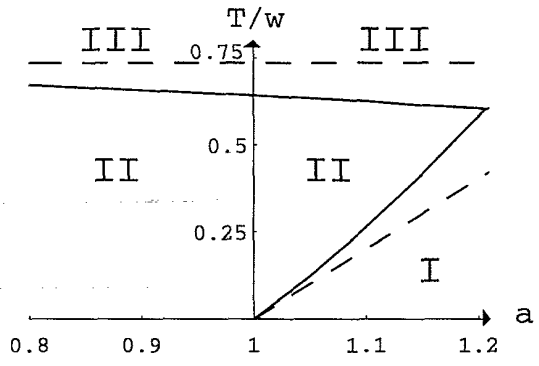


FIG. 3. Phase boundaries for a network of coupled active rotators. The broken curves show the approximated phase boundaries for $w >> a$. The continuous curves show the exact phase boundaries obtained from Eqs. (16) and (17) for $w$=0.25.

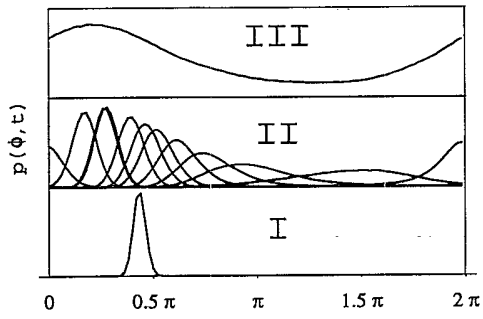


FIG. 4. Distributions of active rotator neurons along the limit cycle for $a = 1.02$, $w = 1$, and $D = 1$ (top), $D = 0.05$, and $D = 0.01$ (bottom) (arbitrary $y$ scale). For $D = 0.05$, distributions are shown for times $0\ (= 53), 1, 2, 6, 21, 42, 48, 50, 51$, and 52 (peaks from left to right). For $D = 0.01$ or 1, the distributions are stationary.

obtained in [14].) In the limit we considered ($w \gg a$), the behavior of the system according to Eqs. (16) and (17) depends only on the value of $a$ and on the ratio $D/w$. We can thus draw a phase diagram analogous to the one obtained in [14] for the different dynamical modes of the system of coupled active rotators (Fig. 3).

Figure 3 shows three different regions in the phase space. In region I, individual neurons fire stochastically at a low average firing rate. The firing among different neurons is uncorrelated. As we increase the noise level or increase the external stimulation of the cell (by lowering the value of $a$), we enter region II, which is characterized by high frequency, synchronous, and periodical firing. As we increase the noise level further or decrease the interaction strength, we enter region III, upon which the firing pattern changes from high frequency correlated firing to high frequency uncorrelated firing. It should be pointed out that while a continuous transition is possible directly from phase I to phase III, these two phases are separated by different transitions from phase II and can be characterized by their low or high firing rate, respectively.

Figure 4 illustrates the probability distributions found in the three regions of the phase space: In region I, a highly localized stationary distribution, and in region II, a time-dependent localized distribution, and in region III, a stationary nonlocalized distribution. It should be pointed out that the stationary distributions in regions I and III correspond to low frequent and high frequent uncorrelated firing activity, respectively.

## VII. CONCLUSIONS

We have argued that in order to study the firing characteristics of neurons, it might be more appropriate to start from a description in terms of stochastic excitable elements rather than from an oscillator description. We have seen that the analytical treatment of excitable element neurons can be simplified by focusing on its dynamics along its stochastic limit cycle, which can be modeled in terms of the active rotator model.

In order to describe the synchronous firing of interacting excitable neurons, we have developed a method that allows us to describe the collective escape of an ensemble of interacting systems out of a local minimum, a method, that should be useful in a series of related problems.

By applying the method to active rotator neurons, we were able to derive the phase boundaries between the phases of synchronous and asynchronous firing activities. Our results have a couple of consequences for the modeling and understanding of synchronous activity in networks of neurons: Figure 3 shows the importance of considering full neuronal dynamics rather than assuming oscillator dynamics from the beginning: if one bases a network model on a description of neurons as oscillators, one is restricted to the left side of Fig. 3, where only one of the two phase transitions occurs.

In excitable systems we thus observe two phase transitions: In the "low noise" transition, I↔II, noise can actually induce synchronous oscillatory behavior, while in the "high noise" transition, II↔III, noise will lead to a loss of coherency. It might be possible to observe both kinds of transitions in biological neural networks. The noise level should probably be treated as a constant in a given biological system; then, the first transition between I and II would be triggered by changes in the excitability of the neurons (parameter $a$), while the second transition between II and III would be triggered by changes in the synaptic efficacies $w$. Due to the different characters of the transitions, Hopf vs saddle-node [12,14,25], crossing the first phase boundary (I→II) leads to a fast, discontinuous increase in firing correlation, while crossing the second phase boundary leads to a gradual, continuous change of firing correlation.

If firing correlation is to play a role in fast recognition processes in the visual cortex, it should be a transition of the first type (I→II). This would mean the physiologically plausible implication, that the same parameter $a$, which modulates the firing frequency of a single neuron in a sigmoidal fashion, would also be responsible for triggering the onset of synchronicity in networks of coupled neurons. It is not yet clear whether networks that process input coming from the visual cortex are actually sensitive to varying degrees of firing correlation among the neurons of the visual cortex. Since the synchronization transition triggered by variations of the synaptic input $a$ is always accompanied by a discontinuous increase in the firing frequency, the phase transition could well be significant for cortical information processing even by merely acting as a signal amplifier which would lead to contrast enhancing between cortical regions that are subcritically stimulated and those that are strongly stimulated with $0 < a < a_c$.

## ACKNOWLEDGMENTS

This work was supported by the National Institute of Health's Resource for Concurrent Biological Computing (Grant No. P41RR05969). Tom Heskes provided numerous useful comments and suggestions on an earlier version of this manuscript.

[1] C. M. Gray, P. König, A. K. Engel, and W. Singer, Nature **338**, 334 (1989).
[2] R. Eckhorn *et al.*, Biol. Cybernet. **60**, 121 (1988)
[3] W. Singer, Annu. Rev. Physiol. **55**, 349 (1993).
[4] M. Steriade, D. A. Cormack, and T. J. Sejnowski, Science **262**, 679 (1993).
[5] H. Sompolinsky, D. Golomb, and D. Kleinfeld, Proc. Natl. Acad. Sci. USA **87**, 7200 (1990).
[6] E. Niebur, H. G. Schuster, D. M. Kammen, and C. Koch, Phys. Rev. A **44**, 6895 (1991).
[7] S. H. Strogatz and R. E. Mirollo, J. Stat. Phys. **91**, 613 (1991).
[8] P. König and T. B. Schillen, Neural Comp. **3**, 155 (1991).
[9] Y. Kuramoto, Physica D **50**, 15 (1991).
[10] E. D. Lumer and B. A. Huberman, Phys. Lett. A **160**, 227 (1991).
[11] D. Wang, J. Buhmann, and C. von der Malsburg, Neural Comput. **2**, 94 (1990).
[12] T. Chawanya *et al.*, Biol. Cybernet. **68**, 493 (1993).
[13] W. Gerstner and J. L. van Hemmen, Phys. Rev. Lett **71**, 312 (1993).
[14] S. Shinomoto and Y. Kuramoto, Prog. Theor. Phys. **75**, 1105 (1986).
[15] C. Kurrer, B. Nieswand, and K. Schulten, in *Self-Organization, Emergent Properties, and Learning*, Vol. 260 of *NATO Advanced Study Institute Series B: Physics*, edited by A. Babloyantz (Plenum Press, New York, 1991), pp. 81–85.
[16] C. Kurrer, B. Nieswand, and K. Schulten, in *Artificial Neural Networks*, edited by E. A. Teuvo Kohonen (Elsevier, Amsterdam, 1991), pp. 133–138.
[17] A. L. Hodgkin and A. F. Huxley, J. Physiol. London **117**, 500 (1952).
[18] R. Fitzhugh, Biophys. J. **1**, 445 (1961).
[19] H. Treutlein and K. Schulten, Ber. Bunsenges. Phys. Chem. **89**, 710 (1985).
[20] H. Treutlein and K. Schulten, Eur. Biophys. J. **13**, 355 (1986).
[21] K. Wiesenfeld, D. Pierson, E. Pantazelou, C. Dames, and F. Moss, Phys. Rev. Lett **72**, 2125 (1994).
[22] Y. Kuramoto, Physica A **106**, 128 (1981).
[23] Y. Kuramoto, *Chemical Oscillations, Waves, and Turbulence* (Springer, Berlin, 1984).
[24] The variable $\phi$ parametrizes a limit cycle on a two-dimensional plane. Linear interactions in this plane may lead to nonlinear interactions in $\phi$ space.
[25] H. Sakaguchi, S. Shinomoto, and Y. Kuramoto, Prog. Theor. Phys. **79**, 600 (1988).
[26] A. Szabo, K. Schulten, and Z. Schulten, J. Chem. Phys. **72**, 4350 (1980).
[27] N. G. van Kampen, *Stochastic Processes in Physics and Chemistry* (North-Holland, Amsterdam, 1981).
[28] C. Kurrer and K. Schulten, Physica D **50**, 311 (1991).
[29] C. Kurrer, Ph.D. thesis, University of Illinois at Urbana-Champaign (1994).